

# Elliptical and parabolic totally internally reflecting optical antennas for wireless infrared communications

R. Ramirez-Iniguez and R. J. Green

Optical Antenna Solutions & Warwick University, School of Engineering, Coventry CV4 7AL,  
[esruk@eng.warwick.ac.uk](mailto:esruk@eng.warwick.ac.uk), [rjg@eng.warwick.ac.uk](mailto:rjg@eng.warwick.ac.uk)

*In the present paper the design and use of nonimaging totally internally reflecting concentrators with elliptical and parabolic front surfaces is discussed, as well as their applications for optical wireless communications. Limitations of a wireless infrared (IR) link are explained, and the use of optical bandpass filters to achieve a high signal-to-noise ratio in a direct detection receiver is described. Properties and design methods of traditional and non-hemispherical nonimaging totally internally reflecting optical antennas are explained. Experimental results of semi-hemispherical totally internally reflecting optical antennas are presented. Finally, comparisons of size, geometrical concentration and maximum output angle of a variety of totally internally reflecting optical antennas are carried out.*

## INTRODUCTION

Three major factors that limit the data transmission rate in an optical wireless link are: multipath distortion (specially significant in some configurations), ambient light, and LED transient time. In most wireless IR systems, the receiver photodetector is not just exposed to the radiation from the transmitter, but also to ambient illumination from lamps or sunlight that have a fraction of energy in the infrared part of the spectrum [1-3]. The three most common sources of light are florescent lamps, incandescent lamps and sunlight, which have a spectral power density as shown in Fig. 1

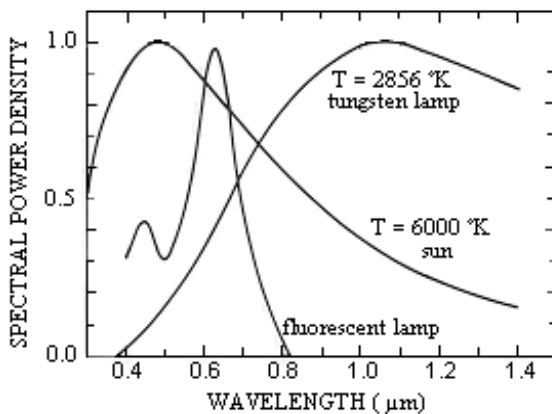


Fig. 1 Spectral power densities of three common ambient light sources [4]

The effect of these three sources of light can be considerably reduced by restricting the field-of-view (FOV) of the receiver and by using optical filters before detection by the photodiode. These filters can be either longpass or bandpass. Longpass filters are the most commonly used in commercial IR systems, as their transmission characteristics are independent of the angle of incidence. To a great extent, the main function of this kind of filter is the restriction of light before the cut-off wavelength. When combined with a silicon photodiode they perform jointly as a bandpass filter (See Fig.2).

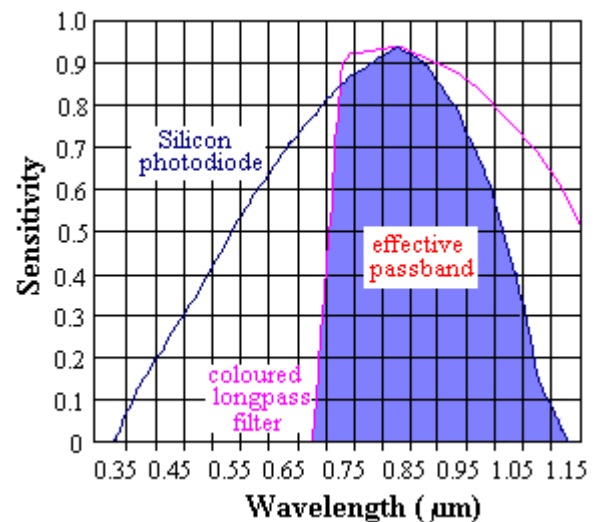


Fig. 2 Spectral sensitivity of Si photodiode and transmittance of a longpass filter [5]

The other option to reduce the ambient light in an optical wireless link is the use of a thin-film bandpass filter. This kind of filter is highly dependent on the angle of incidence and this has to be taken into account when designing the optical front-end of a wireless IR receiver.

Also, optical wireless links suffer from a high path loss that affects the received electrical signal-to-noise ratio (SNR). For instance, in a system using Intensity Modulation/Direct Detection (IM/DD) as the transmission-detection technique, the electrical SNR is proportional to the square of the received optical power. Thus, the receiver must collect as much energy as possible.

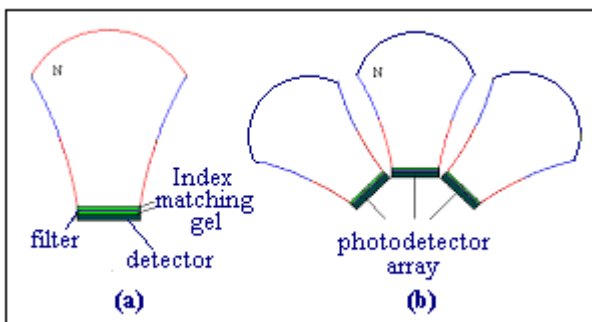
A solution would be to increase the transmitted optical power, but in many cases it is limited due to eye safety and power budget constrains [6]. Another solution would be to use a large area detector, but the problem with these devices is that they have a large capacitance that leads to a reduction of receiver bandwidth and affects the receiver thermal noise directly [7].

Therefore it is desirable to use an optical concentrator to improve the collection efficiency of the receiver by transforming light rays incident over a large area into a set

of rays that emerge from a smaller area. This implies that smaller detectors can be used, which decreases the capacitance, the cost, and improves receiver sensitivity. Furthermore, it is desirable to use transmitters with narrow optical spectrum to allow the receiver to employ a narrowband optical filter to reject ambient light radiation and other sources of noise. It has been demonstrated recently that the use of omnidirectional and directed concentrators used in conjunction with multilayer bandpass filters effectively screen out unwanted ambient radiation and increase the effective area of the photodetector. Examples of nonimaging concentrators used with thin-film bandpass filters are the hemispherical concentrator [8-10] and the Compound Parabolic Concentrator (CPC) [11, 12].

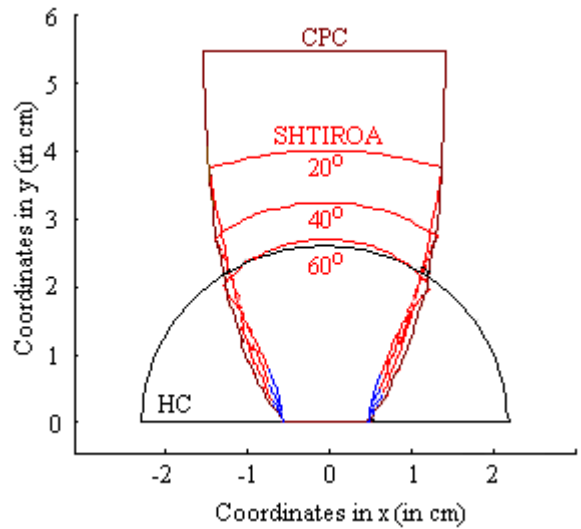
**SEMI-HEMISPHERICAL OPTICAL ANTENNAS**

It has been discussed in previous papers [13-14] how a way of approaching the thermodynamic limit of optical concentration without incurring an excessive length is by using a rotationally-symmetric, three-dimensional, dielectric totally internally reflecting optical antenna. This sort of device achieves very high concentrations because it combines front surface refraction with total internal reflection from its sidewall. Compared to hemispherical concentrators, Semi-Hemispherical totally internally reflecting optical antennas (SHTIROAs) offer higher concentrations, the possibility of designing it for any FOV (which, as it has been explained above, reduces the noise due to background illumination) and the possibility of using flat thin-film optical filters that are easier to fabricate and allow the manufacture process to be relaxed. Compared with CPCs, SHTIROAs have two advantages: smaller size (the size of a SHTIROA can be nearly 1/5 of that of a single dielectric CPC if the front surface arc angle is large enough), and higher concentration. This is because of the use of a curved front surface at the entrance of the concentrator and the large refractive index of the dielectric materials. Figure 3 shows a side view of a variety of structures combining a DTIRC with thin-film optical filters. Fig. 3(a) shows the cross-sectional view of an Optical Antenna comprising a semi-hemispherical dielectric totally internally reflecting concentrator, a thin-film optical filter, a photodetector, and index matching gel. Fig. 3(b) shows a photodetector array structure with a number of optical antennas oriented in different directions.



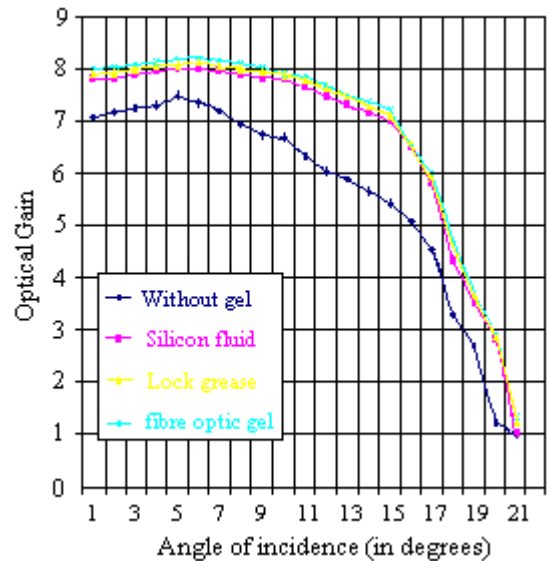
**Fig. 3 Cross-sectional view of (a) a Semi-Hemispherical Optical Antenna, and (b) an Optical Antenna array**

Figure 4 shows different concentrator design superimposed on each other. It can be seen here how as the front surface arc angle of a SHTIROA is increased (from 0° which is the specific case of a CPC, to 60°), the size of the concentrator becomes smaller.



**Fig. 4 Comparison of concentrators size**

A typical optical gain response of a SHTIROA as the angle of incidence varies from 0° to the critical angle is shown in Fig. 5



**Fig. 5 Typical optical gain response with angle of incidence (for an Optical Antenna attached with different index matching gels)**

**PTIROA and ETIROA**

The effect of the variation of the front surface arc angle on the gain, the total height and the maximum output angle of the SHTIROA has been presented and analysed in previous papers. The results obtained suggest that the DTIRC may benefit from the choice of an aspherical front surface because of its high effect on the output parameters. For this purpose, two different geometrical curves have been chosen to compare their performance with that of the SHTIROA: a parabola and an ellipse.

The design of the parabolic TIROA is based on the same principles that are used for the SHTIROA, but it is slightly more complicated.

In a traditional SHTIROA the slope of the side profile is set to values that allow the condition of total internal reflection (TIR). Also, it is necessary to take into account other subsidiary conditions that may have been imposed. For instance, rays may also be required to exit the concentrator with an angle not exceeding a certain value if an interference filter is going to be used between the concentrator and the photodetector. The designer will have to decide whether the concentration or the filtering have priority, or make a compromise between them. The side profile can be divided into two parts: P1-P2 and P2-P3. Extreme rays refracted and directed to the part P1-P2 are reflected to the corner P3' after a single reflection. Rays reflected at P2 satisfy the condition of TIR just barely and exit from P3'. Reflected rays from the part (P2-P3) exit the concentrator forming a new wavefront (see Fig. 6).

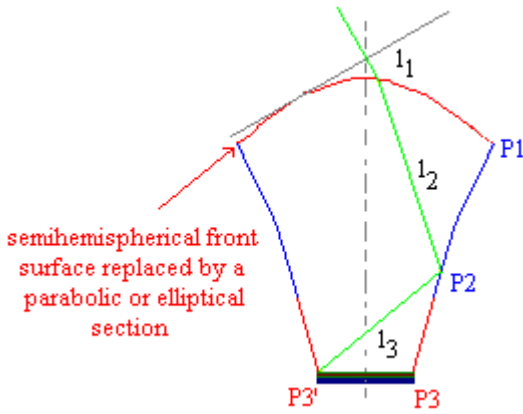


**Fig. 6 Optical path length sections of the PTIROA**

The general SHTIROA design method is based on the geometrical wavefront definition, which implies that the total optical path length is a constant for every ray that connects the initial and the final wavefronts.

As it is impossible to define a front surface arc angle in the same way it is done for the SHTIROA (simply defining it as an input parameter), the parabola height and diameter are chosen as the input parameters. Then, by placing the curve base in the  $x$ -axis and its centre in the  $y$ -axis, the  $p$  parameter can be obtained from the equation of a parabola with the aperture facing down and with the vertex in the coordinate  $(0, \text{parabola height})$  as follows:

$$(x - x_0)^2 = -2p(y - y_0) \quad (1)$$

where  $x_0$  and  $y_0$  are the coordinates of the vertex. Thus,

$$p = \frac{\left(\frac{d_1}{2}\right)^2}{2h_{pa}} \quad (2)$$

Here,  $d_1$  is the trial entrance diameter of the concentrator and  $h_{pa}$  is the parabola height. Once the  $p$  parameter has been found, it is possible to obtain the  $y$  coordinates of the parabola in that position as follows:

$$y_{initial} = -\frac{x^2 - 2ph_{pa}}{2p} \quad (3)$$

where the  $x_{initial}$  coordinates are assigned according to the desired numerical precision. This is done by gradually increasing the value of the  $x_{initial}$  position between  $-d_1/2$  and  $d_1/2$ . This creates the  $x$  vector used to calculate the vector for the  $y$  position.

After the parabolic surface has been defined, an "equivalent" front surface arc angle can be obtained. A line which joins the first two points of the parabola with respect to the  $x$ -axis forms this angle, and it is equivalent to the maximum arc angle  $\theta$  used to define the incident ray positions in the semi-hemispherical DTIRC. The importance of the equivalent front surface arc angle is that it helps to define the maximum refracted angle with respect to the vertical axis, and thus the profile height. It also helps as a point of reference to compare the different concentrators. In an equivalent way to the SHTIROA, the maximum refracted angle can be calculated as:

$$\theta'_{max} = \sin^{-1}\left(\frac{\sin(\theta_a - \varphi)}{n}\right) + \varphi \quad (4)$$

where  $\varphi$  is the equivalent front surface arc angle,  $\theta_a$  is the acceptance angle of the concentrator, and  $n$  is its index of refraction. The profile height can subsequently determined using the formula below:

$$H = \frac{d_1 + d_0}{2} \cot(\theta'_{max}) \quad (5)$$

With the height that has been obtained, the real front surface coordinates can be calculated as follows:

$$x = x_{initial} \quad (6)$$

$$y = y_{initial} + H \quad (7)$$

As it can be seen, the complexity of this method derives from the fact that the concentrator front surface is not as straightforward to define as it is in the semi-hemispherical one, but once this parabolic surface has been defined, the coordinates of the concentrator profile can be calculated in a very similar way to the one for the SHTIROA.

In the case of the Elliptical Totally Internally Reflecting Optical Antenna (ETIROA) the first step in its design is to define the front surface. Unlike its parabolic and semi-hemispherical counterparts, the ETIROA requires 2 parameters to be defined: the ellipse height  $b$ , and the ellipse half base  $a$ , as shown in Fig. 7.

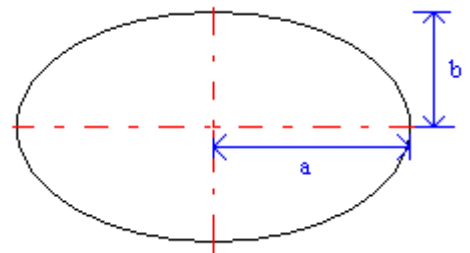


**Fig. 7 Ellipse defining parameters**

The other parameters the program needs in order to define the concentrator are: the index of refraction of the concentrator material, the exit aperture (the diameter of the detector), the acceptance angle, the numerical precision and a trial entrance diameter.

Before calculating the concentrator profile coordinates, the program first generates the points (on the positive side of the y axis) of the ellipse according to formula 8 (ellipse with axis intersection at the origin) at increments in x defined by the numerical precision.

$$\frac{x^2}{a^2} + \frac{y^2}{b^2} - 1 = 0 \quad (8)$$

After the original ellipse has been generated, it is possible to define the part of the ellipse that will be used, i.e. the part that is contained within the defined entrance diameter. It is impossible to use the ellipse as originally defined because this would be equivalent to the use of a hemispherical DTIRC with  $\varphi = 90^\circ$  for which designs are physically impossible.

The equivalent front surface arc angle can be calculated from the first two points of the ellipse section. Also, the maximum refracted angle can be calculated with the obtained equivalent front surface arc angle and the acceptance angle, as is shown in expression 4. Once this angle has been obtained, the profile height can be calculated with expression 5, and the front surface coordinates can be redefined as follows:

$$x = x_{initial} \quad (9)$$

$$y = y_{initial} - y_{initial}(1) + H \quad (10)$$

where  $y_{initial}(1)$  is the y coordinate of the first point of the ellipse. As in the parabolic case, the concentrator coordinates are more difficult to generate, due to the fact that the elliptical front surface cannot be defined as easily as for the semi-hemispherical TIROA.

## TIROAs COMPARISON

As explained above, the reason why an equivalent front surface arc angle is produced for the elliptical and the parabolic DTIRC is to facilitate the comparison between the different DTIRC designs.

The use of the same equivalent arc angle in the comparison graphs ensures that the maximum angle refracted on the front surface and the maximum output angle are the same for all the designs. This means that for the graphs presented in the next figures, the differences between the size and the geometrical gain of the different DTIRCs are shown for the same maximum output angle.

The first thing that can be observed in the next graph (Fig. 8) is that the variation in size for the different DTIRC designs is generally small (and the variation of the output parameters -the gain, the maximum output angle and the size- is similar in the rest of the graphs too). It can also be observed that the TIROA design that provides the smallest size is the elliptical one, while the parabolic TIROA is the largest concentrator in the majority of the graphs.

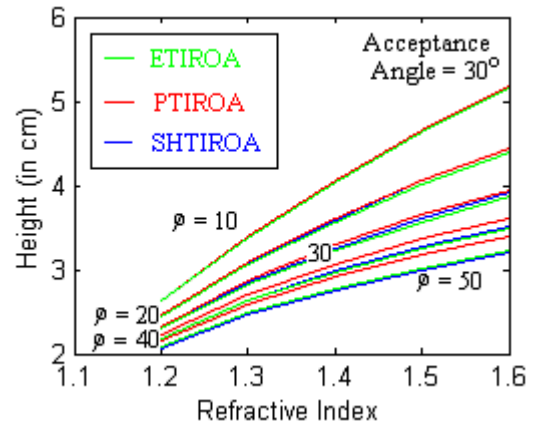


**Fig 8 Size comparison between ETIROA, PTIROA and SHTIROAs for different arc angles**

Whereas the PDTIRC becomes larger than the SHDTIRC as the front surface arc angle increases, the EDTIRC becomes smaller for small arc angles and larger for big ones.

The difference in size between the three DTIRC designs is also presented in Fig. 9. Here it can be observed how the difference in size between the DTIRCs becomes bigger as the equivalent arc angle is made larger.

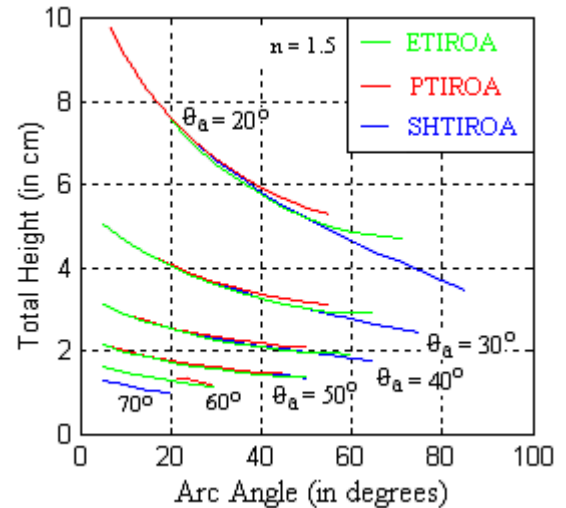


**Fig. 9 Size comparison between ETIROA, PTIROA and SHTIROA for different acceptance angles**

This is logical considering the fact that the smaller the arc angle is, the more all the design look like a compound parabolic concentrator. An interesting aspect is that for small acceptance angles the elliptical TIROA has a small size, whereas it becomes larger than the SHTIROA for higher ones.

The comparison of the gain between the different DTIRCs is presented in Figs. 10 and 11. Here, as expected, the bigger size of the parabolic DTIRC is compensated by a larger gain (Fig. 10).

It is interesting to notice how, for the front surface arc angle values that make the PTIROA and the ETIROA larger than the SHTIROA, the gain values are also increased. For values of the EDTIRC arc angle where the total height is smaller than the one for the SHTIROA, the geometrical gain is lower as well.

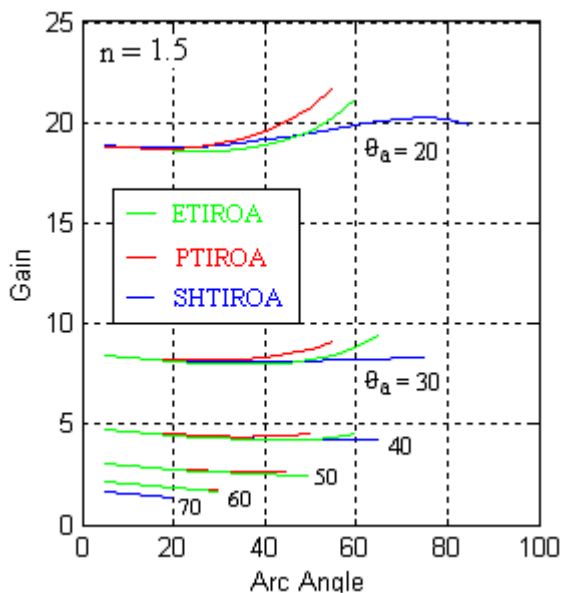


**Fig. 10 Gain comparison between ETIROA, PTIROA and SHTIROA for different acceptance angles**

Fig. 11 shows the variation of the gain with the acceptance angle for the different DTIRC's at different indices of refraction and for a front surface arc angle of  $50^\circ$ .

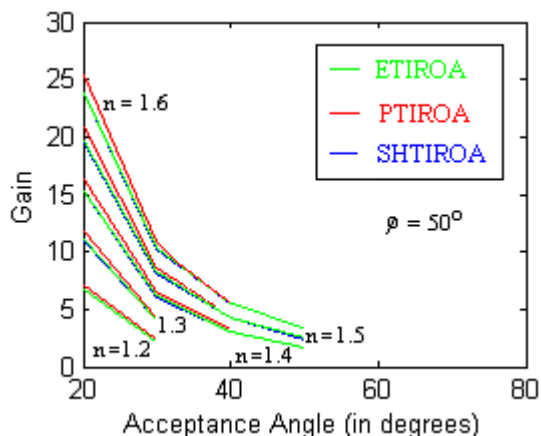


**Fig. 11 Gain comparison between ETIROA, PTIROA and SHTIROA for different acceptance angles**

## CONCLUSIONS

In this paper, different modifications to the original Optical Antenna (SHTIROA) have been introduced. First, the design of TIROAs with front surfaces that differ from the semi-hemispherical one shown in previous papers has been presented. Then, design procedures for parabolic TIROAs have been explained, followed by a design method for the elliptical TIROAs.

Next, comparisons between the different types of TIROAs have been made. Here it could be seen that, although for the same input parameters (and maximum output angles) the PTIROA presents a larger size than the SHTIROA, it also offers the advantage of a higher gain. Furthermore, it could be noticed that, depending on the value of the front-surface arc angle, the elliptical TIROA can offer lower or higher gains with corresponding smaller or larger sizes than the SHTIROA.

It can be concluded that the use of one TIROA or another in an optical wireless link depends to a great extent on the application in which they will be used. If minimum size is required, an elliptical TIROA with a low front surface arc angle can be used, and if maximum concentration is required, a parabolic TIROA is the best option.

## REFERENCES

- [1] R. T. Valadas and A. M. de Oliveira Duarte, "Sectorized Receivers for Indoor Wireless Optical Communication Systems," *IEEE International Conference in Communications*, pp. 1090-1095, 1994.
- [2] A. Boucouvalas, "Indoor ambient light noise and its effect on wireless optical links," *IEE Proceedings in Optoelectronics*, vol. 143, no. 6, pp. 334-338, December, 1996.
- [3] A. J. C. Moreira, R. T. Valadas, and A. M. de Oliveira Duarte, "Performance of infrared transmission systems under ambient light interference," *IEE Proceedings in Optoelectronics*, vol. 143, no. 6, pp. 339-346, December, 1996.
- [4] J. R. Barry, J. M. Kahn, E. A. Lee, and D. G. Messerschmitt, "High-Speed Nondirective Optical Communication for Wireless Networks," *IEEE Network Magazine*, pp. 44-54, 1991.
- [5] F. R. Gfeller and U. H. Bapst, "Wireless In-House Data Communication via Diffuse Infrared Radiation," *Proceedings of the IEEE*, vol. 67, pp. 1474-1486, 1979.
- [6] J. J. G. Fernandes, P. A. Watson, and J. C. Neves, "Wireless LANs: Physical Properties of Infra-Red Systems vs. Mmw Systems," *IEEE Communications Magazine*, pp. 68-73, August, 1994.
- [7] R. Ramirez-Iniguez, S. M. Idrus, and R. J. Green, "Receiver Amplifiers for Optical Wireless Communication Systems," *PREP2001*, Keele University, UK, pp. 19-20, 17-18 April, 2001.
- [8] J. P. Savicki and S. P. Morgan, "Hemispherical concentrators and spectral filters for planar sensors in diffuse radiation fields," *Applied Optics*, vol. 33, no. 34, pp. 8057-8061, December, 1994.
- [9] M. E. Marhic, M. D. Kotzin, and A. P. Van den Heuvel, "Reflectors and immersion lenses for detectors of diffuse radiation," *Optical Society of America*, vol. 72, no. 3, pp. 352-355, March, 1982.
- [10] J. R. Barry, *Wireless Infrared Communications*: Kluwer Academic Publishers, 1994.
- [11] K. Ho and J. M. Kahn, "Compound parabolic concentrators for narrowband wireless infrared receivers," *Optical Engineering*, vol. 34, no. 5, pp. 1385-1395, May, 1995.
- [12] W. T. Welford and R. Winston, *High Collection Nonimaging Optics*: Academic Press, 1989.
- [13] R. Ramirez-Iniguez and R. J. Green, "Totally internally reflecting optical antennas for wireless IR communication," *IEEE Wireless Design Conference*, London, UK, pp. 129-132, May 2002, 2002.
- [14] R. Ramirez-Iniguez and R. J. Green, "Dielectric Totally Internally Reflecting Concentrators (DTIRC's) for Optical Wireless Receivers," *PREP2002*, Nottingham, pp. Communications Track 4, 17-19 April, 2002.